THE JOURNAL OF BIOLOGICAL CHEMISTRY Vol. 279, No. 47, Issue of November 19, pp. 48808–48818, 2004

Printed in U.S.A.

ErbB4 Expression in Neural Progenitor Cells (ST14A) Is Necessary to Mediate Neuregulin-1β1-induced Migration*

Received for publication, July 23, 2004, and in revised form, August 24, 2004
Published, JBC Papers in Press, September 8, 2004, DOI 10.1074/jbc.M408374200

Giovanna Gambarotta‡§, Donatella Garzotto‡¶, Erika Destro‡¶, Beatrice Mautino‡, Costanza Giampietro‡, Santina Cutrupi‖, Claudio Dati‡, Elena Cattaneo, Aldo Fasolo‡, and Isabelle Perroteau‡**

*From the ‡Department of Human and Animal Biology, University of Torino, Torino 10123, Italy, the ‖Department of Medical Sciences, University of Piemonte Orientale, Novara 28100, Italy, and the **Department of Pharmacological Sciences, University of Milan, Milan 20133, Italy*

Activation of the receptor tyrosine kinase ErbB4 leads to various cellular responses such as proliferation, survival, differentiation, and chemotaxis. Two pairs of naturally occurring ErbB4 isoforms differing in their juxtamembrane (JMa/JMb) and C termini (cyt1/cyt2) have been described. To examine the role of ErbB4 in neuron migration, we cloned and stably transfected each of the four ErbB4 isoforms in ST14A cells (a neural progenitor cell line derived from the striatum of embryonic day 14 rats) endogenously expressing the other members of the ErbB family: ErbB1, ErbB2, and ErbB3. Using immunoprecipitation assays, we showed that the neuregulin-1β1 (NRG1β1) stimulus induced ErbB4 tyrosine phosphorylation and phosphatidylinositol 3-kinase (PI3K) recruitment and activation (as demonstrated by Akt phosphorylation) either directly (ErbB4 cyt1 isoform) or indirectly (ErbB4 cyt2 isoform). We examined the ability of the four ErbB4 isoforms to induce chemotaxis and cell proliferation in response to NRG1β1 stimulation. Using migration assays, we observed that only ErbB4-expressing cells stimulated with NRG1β1 showed a significant increase in migration, whereas the growth rate remained unchanged. Additional assays showed that inhibition of PI3K (but not of phospholipase Cγ) dramatically reduced migratory activity. Our data show that ErbB4 signaling via PI3K activation plays a fundamental role in controlling NRG1β1-induced migration.

The ErbB receptor family consists of four receptor tyrosine kinases named the epidermal growth factor (EGF)[1] receptor, ErbB2, ErbB3, and ErbB4 (reviewed in Ref. 1). Ligand-dependent activation of ErbB receptors results in homo- or heterodimerization, which stimulates receptor *trans*-phosphorylation on cytoplasmic tyrosine residues, creating binding sites for adaptor or enzymatic proteins. EGF receptor and ErbB4 homodimers are active kinases in the absence of coreceptors, whereas ErbB3 (which has little or no intrinsic tyrosine kinase activity) and ErbB2 (for which no ligand has been identified) necessitate coreceptor interaction for signal transduction (2). Thus, whereas ErbB2 and ErbB3 are limited to heterodimerization, the EGF receptor and ErbB4 can be activated by either homo- or heterodimerization.

An interesting ErbB4 feature (recently reviewed in Ref. 3) is the existence of isoforms generated by alternative splicing (4). One isoform pair (5) is characterized by alternative splicing of exons located in the extracellular juxtamembrane region conferring (JMa), or not (JMb), susceptibility to proteolytic cleavage (6) by a member of the ADAM (a disintegrin and metalloprotease) family, the tumor necrosis factor-α-converting enzyme (7). ErbB4 proteolytic cleavage produces a membrane-associated 80-kDa fragment that can be degraded by proteasome activity following polyubiquitination (8) or that can be the substrate for subsequent γ-secretase cleavage, which releases the cytoplasmic domain from the membrane and allows, intriguingly, nuclear translocation of a fragment (9, 10) that can act as cotranscriptional activator of the Yes-associated protein (11, 12).

The other ErbB4 isoform pair (13) is characterized by the presence (cyt1) or absence (cyt2) of a cytoplasmic exon containing a docking site for phosphatidylinositol 3-kinase (PI3K). The existence of these isoforms suggests that potentially four isoforms may exist and evoke functional differences. Actually, in stable NIH3T3 transfectants, it has been shown that the ErbB4 isoform that does not activate PI3K (cyt2) mediates proliferation, but not survival or chemotaxis, as does cyt1 (13).

ErbB4 ligands belong to two groups: the neuregulins (NRG1–4), also termed heregulins, and some members of the EGF family (betacellulin, epiregulin, and HB-EGF). NRG1 and NRG2 exist in a number of splicing isoforms and recognize also ErbB3 as a binding site, whereas NRG3 and NRG4 interact, with lower affinity, only with ErbB4 (1). In most assays, NRG1 with a β-type EGF-like domain is 10–100 times more potent than NRG1 with an α-type EGF-like domain. Moreover, experiments performed with mice with targeted mutations showed that NRG1β is involved in nervous system and cardiac development, whereas NRG1α is involved in breast development (reviewed in Ref. 14).

In the central nervous system, NRG1 is expressed by both neurons and glia (15–17), and ErbB4 is expressed in various part of the brain and nervous system (18–22), including the

* This work was supported by a grant from the Compagnia di S. Paolo, (Grant MIUR-PRIN 2001), and PRONEURO (Grant FIRB RBNE01WY7P). The costs of publication of this article were defrayed in part by the payment of page charges. This article must therefore be hereby marked "*advertisement*" in accordance with 18 U.S.C. Section 1734 solely to indicate this fact.

The nucleotide sequence(s) reported in this paper has been submitted to the GenBank™/EBI Data Bank with accession number(s) AY375306, AY375307, and AY375308.

§ To whom correspondence should be addressed: Dipt. di Biologia Animale e dell'Uomo, Università degli Studi di Torino, Via Accademia Albertina 13, 10123 Torino, Italia. Tel.: 39-11-670-4688; Fax: 39-11-670-4692; E-mail: giovanna.gambarotta@unito.it.

¶ Both authors contributed equally to this work.

[1] The abbreviations used are: EGF, epidermal growth factor; PI3K, phosphatidylinositol 3-kinase; NRG, neuregulin; HB-EGF, heparin-binding epidermal growth factor-like growth factor; DMEM, Dulbecco's modified Eagle's medium; FBS, fetal bovine serum; PBS, phosphate-buffered saline; RT, reverse transcription; t, time; GAPDH, glyceraldehyde-3-phosphate dehydrogenase.

retina (23), the hippocampus (24, 25) and, as we (26, 27) and others (22) have previously shown, the olfactory bulb. Interestingly, cells coming out of the rostral migratory stream of the subependymal layer as well as isolated cells in the granule cell layer, possibly migrating cells, strongly express ErbB4, and ErbB4 immunoreactivity is found in all the periglomerular and mitral/tufted cells of the olfactory bulb (26, 28). Furthermore, ErbB4 is preferentially expressed by interneurons that migrate tangentially from the ventral to the dorsal rat telencephalon (29). ErbB4 knockout mice exhibit defects in cranial neural crest migration and cranial nerve segregation in the developing hindbrain, but die at embryonic day 10.5 because of abnormal heart development (30, 31). Recently, heart defects were rescued in mutant ErbB4 mice by expressing ErbB4 under the control of a cardiac-specific myosin promoter (32). Rescued mice display aberrant cranial nerve architecture and an increased number of large interneurons within the cerebellum. Expression of a dominant-negative ErbB4 construct in primary cultures of neuronal cells showed an additional ErbB4 requirement for cell migration in the developing cerebellum: the phenotype described includes defects in the migration of cerebellar granule cells (expressing NRGs) along radial glial fibers (usually expressing ErbB4) (33).

All of this evidence concerning a role for ErbB4 in cell migration in the nervous system prompted us to find a suitable *in vitro* model in which to investigate more deeply the involvement of ErbB4 in migration. For this purpose, we chose ST14A, an ErbB1/ErbB2/ErbB3-expressing cell line derived from embryonic day 14 rat striatal primordia by retroviral transduction of a temperature-sensitive allele of the SV40 large T antigen (34). In this model, cell division and expression of nestin persist at 33 °C, the permissive temperature, whereas at the non-permissive temperature of 39 °C, cell division ceases, nestin expression decreases, and microtubule-associated protein-2 expression increases (35). Unlike cells derived from somatic fusion (36), they contain a normal complement of chromosomes without contamination from a neuroblastoma cell line. Following intracerebral grafting procedures, ST14A cells develop into a high percentage of microtubule-associated protein-2- and glial fibrillary acidic protein-positive cells, suggesting that they behave as multipotent neural progenitors (37). These properties, together with the stability of their phenotype over several years since derivation, associated with the feasibility of their engineering and subcloning, identify them as an appropriate model for molecular and biochemical investigations of gene function (38–40).

In this study, we engineered ST14A cells to express ErbB4 and demonstrate that ErbB4 expression is necessary to confer on neural progenitor cells the ability to respond to NRG1β1 through migration. This response is shown to be mediated by PI3K activation either directly or indirectly through ErbB3 heterodimerization.

EXPERIMENTAL PROCEDURES

Cell Culture and Reagents—All chemicals and reagents were purchased from Sigma unless otherwise stated. COS-7 cells were purchased from and maintained as recommended by American Type Culture Collection.

The ST14A cell line was derived from primary cells dissociated from embryonic day 14 rat striatal primordia and conditionally immortalized by retroviral transduction of the temperature-sensitive variant tsA58/U19 of the SV40 large T antigen (34). Cells were cultured on dishes (BD Biosciences) in Dulbecco's modified Eagle's medium (DMEM) supplemented with 100 units/ml penicillin, 0.1 mg/ml streptomycin, 1 mM sodium pyruvate, 2 mM L-glutamine, and 10% heat-inactivated fetal bovine serum (FBS; Invitrogen). Stable transfectants were grown in medium containing 5 μg/ml puromycin (Sigma). Cells were grown as monolayers at the permissive temperature of 33 °C in a 5% CO_2 atmosphere saturated with H_2O. Cells were allowed to grow to near confluence, and adherent cells were harvested by the trypsin/EDTA method.

The EGF-like domain of mouse NRG1β1 was produced in our laboratory as a His-tag fusion protein in *Escherichia coli* (41). The PI3K inhibitor LY294002 was dissolved in dimethyl sulfoxide (20 mM stock solution) and stored at −20 °C. The phospholipase Cγ inhibitor U73122 was dissolved in chloroform according to the manufacturer's instructions to a final concentration of 2 mM, divided in aliquots, lyophilized, stored at −20 °C, and resuspended in dimethyl sulfoxide just before use to obtain a 2 mM stock solution. In all experiments, control samples received the same concentration of dimethyl sulfoxide or other vehicle.

Polyclonal anti-ErbB4 (C-18, sc-283) and monoclonal anti-phosphotyrosine (PY99) primary antibodies were from Santa Cruz Biotechnology. Polyclonal anti-PI3K p85 antibody was from Upstate Biotechnology, Inc. Polyclonal anti-phospho-Ser^{473} Akt and anti-Akt antibodies were from Cell Signaling. Horseradish peroxidase-linked donkey anti-rabbit and sheep anti-mouse secondary antibodies were from Amersham Biosciences.

Proliferation Assay—The proliferation assay was performed according to the protocol described by Kueng *et al.* (42). Briefly, cells were plated in 200 μl of DMEM containing 10% FBS at a density of 1000 cells/well in 96-well plates. The following day ($t = 0$), the medium was replaced with 2% FBS-containing DMEM with or without 5 nM NRG1β1 (100 μl/well, 8 wells/treatment). For each plate, an 8-well line without cells was treated as the entire plate and used as a blank in the following microplate reader analysis. At $t = 0$, a 96-well plate was fixed and used as a cell growth starting point. Cell growth was subsequently calculated at 2 ($t = 48$ h), 4 ($t = 96$ h), and 6 ($t = 144$ h) days after the initiation of treatments. Briefly, the medium was removed, and cells were fixed by addition of 100 μl of 2% glutaraldehyde in phosphate-buffered saline (PBS). After being shaken (200 cycles/min) for 20 min at room temperature, plates were washed five times by submersion in deionized water and air-dried for at least 24 h. Plates were then stained by addition of a solution (100 μl/well) containing 0.1% crystal violet dissolved in freshly prepared 200 mM boric acid (pH 9.0). After being shaken (200 cycles/min) for 20 min at room temperature, plates were washed five times by submersion in deionized water and air-dried for at least 24 h. Bound dye was solubilized by addition of 10% acetic acid (100 μl/well) and 5 min of shaking at room temperature. The absorbance of dye extracts was measured directly in plates using a Microplate Reader (Bio-Rad) at a wavelength of 590 nm.

Reverse Transcription (RT)-PCR and Cloning of Rat ErbB4 cDNAs—Total RNA was prepared from olfactory bulbs obtained from one adult Wistar rat (Charles River Laboratories) using the TRIzol reagent (Invitrogen) according to the manufacturer's instructions. Total RNA (1 μg) was subsequently reverse-transcribed to cDNA in a total volume of 25 μl using 200 units of reverse transcriptase (U. S. Biochemical Corp.) in 1× buffer (U. S. Biochemical Corp.) with 7.5 μM random exanucleotide primers (Amersham Biosciences), 0.05% Triton X-100, 0.5 mM dNTPs (Amersham Biosciences), 0.1 μg/μl acetylated bovine serum albumin (Amersham Biosciences), and 33 units of RNasin (Amersham Biosciences). As a control, an enzyme-less reaction was performed for each sample. PCRs were carried out in a total volume of 50 μl containing 5 μl of cDNA, enzyme-less reaction sample, or water (negative controls), 250 nM each 5′- and 3′-primers (see below), 2.5 units of *PfuTurbo*® DNA polymerase (Stratagene), 100 μM dNTPs, and 5% glycerol. The primers used (produced by Sigma) were designed according to the GenBank™/EBI rat ErbB4 sequence (accession number NM_021687; corresponding to the JMa-cyt1 isoform, herein numbered considering the start site as +1): primer ErbB4-11 (5′-TGCTAGCCAAAA**ATG**AAGCTGGCG-3′, with the artificial NheI site underlined and the ATG codon in boldface) and primer ErbB4-4 (5′-GTTTCTCCTTCAGGTACCCAGATTCC-3′) to obtain the amplicons corresponding to nucleotides −7 to +2228 and primer ErbB4-5 (5′-GCACAGCACCCAATCAAGCTC-3′) and primer ErbB4-6 (5′-TACTGGCCTTGGGGTAGAAGGAAG-3′) to obtain the amplicons corresponding to nucleotides +2105 to +4025. Samples were amplified using a simplified touchdown PCR protocol: denaturation at 95 °C for 5 min; followed by 10 cycles of denaturation at 95 °C for 30 s, annealing at 66 °C for 30 s, and extension at 72 °C for 3 min; followed by 30 cycles of denaturation at 95 °C for 30 s, annealing at 57 °C for 30 s, and extension at 72 °C for 3 min. The extension step of the last cycle was increased to 30 min. PCR products were separated by electrophoresis on a 0.8% agarose gel, stained with ethidium bromide, and visualized with UV light. A 1-kb DNA ladder (Invitrogen) or BenchTop pGEM DNA markers (Promega) was used as a size marker. PCR products were purified from agarose gel using the GenElute™ gel purification kit (Sigma). To obtain the full-length ErbB4 cDNAs, the previously obtained amplicons (nucleotides −7 to

+2228 and nucleotides +2105 to +4025) were used as templates in the presence of primers ErbB4-11 and ErbB4-6 in recombinant PCR according to the following protocol: denaturation at 95 °C for 5 min, followed by 30 cycles of denaturation at 95 °C for 30 s, annealing at 63 °C for 30 s, and extension at 72 °C for 8 min. The extension step of the last cycle was increased to 30 min. PCR products were separated by electrophoresis on a 0.8% agarose gel, purified from agarose gel using the GenElute™ gel purification kit, and cloned into the pCR®-BluntII-TOPO® vector (Invitrogen) using the Zero Blunt® TOPO® PCR cloning kit (Invitrogen) following the manufacturer's instructions.

The DNA of 18 single colonies was obtained using the GenElute™ plasmid miniprep kit (Sigma). For each clone, the orientation of the cDNA in the vector (sense or antisense) was detected by restriction enzyme digestions using EcoRI and BamHI (Amersham Biosciences). To identify the different ErbB4 isoforms (cyt1/cyt2 and JMa/JMb), individual sense clones were analyzed by PCR; the juxtamembrane domain (fragment +1773 to +2019) was amplified with primer ErbB-4-12 (5′-GAAATGTCCAGATGGCCTACAG-3′) and primer ErbB4-13 (5′-AACGGCAAATGTCAGAGCCATG-3′), and the cytoplasmic domain (fragment +3054 to +3267) was amplified with primer ErbB4-1 (5′-TGCTGAGGAATATTTGGTCCCCCA-3′) and primer ErbB4-2 (5′-TCTGGTATGGTGCTGGTTGTGGCT-3′). PCRs were carried out in a total volume of 50 μl containing 5 μl of DNA or water (negative controls), 250 nM each specific primer, 1 unit of RED Taq™ DNA polymerase (Sigma), 100 μM dNTPs, and 5% glycerol. Samples were amplified by denaturation at 95 °C for 3 min, followed by 30 cycles of denaturation at 94 °C for 30 s, annealing at 63 °C (JMa/JMb) or 60 °C (cyt1/cyt2) for 30 s, and extension at 72 °C for 1 min. The extension step of the last cycle was increased to 20 min. To amplify the glyceraldehyde-3-phosphate dehydrogenase (GAPDH) cDNA fragment corresponding to nucleotides 544–732 (GenBank™/EBI accession number M32599), PCRs were carried out using primer GAPDH1 (5′-TGGCATTGTGGAAGGGCTCATTGAC-3′) and primer GAPDH2 (5′-ATGCCAGTGAGCTTCCCGTTCAGC-3′); samples were amplified by denaturation at 95 °C for 3 min, followed by 25 cycles of denaturation at 94 °C for 30 s, annealing at 60 °C for 30 s, and extension at 72 °C for 1 min. PCR products were separated by electrophoresis on 2% agarose gels. For all PCRs, the Thermal Cycler GeneAmp® PCR System 2400 (PerkinElmer Life Sciences) was used.

Sequencing of ErbB4 cDNAs—Two cDNA clones (3A and 3G) corresponding to the full-length JMa-cyt1 and JMa-cyt2 isoforms were completely sequenced on both strands (Genelab Laboratories, Rome, Italy). A cDNA clone (3E) corresponding to the JMb isoform was sequenced on both strands in the region between nucleotides −7 and +2196. The primers used for sequencing were designed according to the GenBank™/EBI rat ErbB4 sequence (accession number NM_021687).

Expression Vectors—To generate stable cell lines expressing ErbB4 JMa-cyt1 and JMa-cyt2, the cDNAs corresponding to the two sequenced isoforms were subcloned into the pIRESpuro2 vector (Clontech); NheI-NotI fragments obtained from pCR®-BluntII-TOPO®-ErbB4 clones (containing the entire rat ErbB4 cDNAs) were subcloned into the NheI and NotI sites of pIRESpuro2. To generate stable cell lines expressing ErbB4 JMb-cyt1 and JMb-cyt2, a Csp45I-HpaI fragment containing the entire juxtamembrane region was obtained from the JMb-sequenced clone and used to replace the JMa region in clones pIRESpuro2-ErbB4-JMa-cyt1 and pIRESpuro2-ErbB4-JMa-cyt2, yielding pIRESpuro2-ErbB4-JMb-cyt1 and pIRESpuro2-ErbB4-JMb-cyt2, respectively. The rat ErbB3 expression vectors pcDNA3-B3 (43) and pcDNA3-B3-6F (44), in which codons corresponding to Tyr^{1051}, Tyr^{1194}, Tyr^{1219}, Tyr^{1257}, Tyr^{1273}, and Tyr^{1286} were substituted with phenylalanine codons, were a generous gift of Dr. John G. Koland (Department of Pharmacology, University of Iowa, College of Medicine, Iowa City, IA).

Transfections—For stable transfections, growing ST14A cells were transfected in triplicate with 10 μg of DNA for each construct using 20 μl of LipofectAMINE and Opti-MEM I (Invitrogen) according to the manufacturer's recommendations. DNA was prepared using the GenElute™ endotoxin-free plasmid maxiprep kit (Sigma). Cells transfected with the pIRESpuro2 vector alone were generated to be used as controls. Cells were cultured in DMEM as described above; and 48 h after transfection, three different doses of puromycin (5, 10, and 20 μg/ml) for each construct were added to the three plates. Individual clones were recovered and screened for their ErbB4 expression level by Western blotting as described below.

For transient transfections, growing COS-7 cells were transfected using specific combinations of expression plasmids as indicated. Briefly, 5 μg of each plasmid were mixed in 1 ml of PBS and added to 1 ml of PBS containing 800 μg/ml DEAE-dextran. COS-7 cells were washed twice with 10 ml of PBS, covered with the DNA/DEAE-dextran/PBS solution, and incubated for 40 min at 37 °C. Then, 10 ml of DMEM containing 10% FBS and 0.1 mM chloroquine were added to the cells, and the cells, spontaneously detached after severe resuspension, were split in two and incubated at 37 °C for 3 h. After removing the medium, cells were treated for 3 min with DMEM containing 10% FBS and 10% Me_2SO, washed once with DMEM, and finally covered with DMEM containing 10% FBS. Twenty-four hours after plating, the cells were washed with PBS and serum-starved in DMEM for an additional 24 h before NRG1β1 stimulation.

Immunoprecipitation and Western Blotting—For immunoprecipitation experiments, confluent cells grown on 10-cm dishes were serum-starved overnight. The following day, 1 mM sodium orthovanadate was added to both the untreated and treated cells for at least 30 min prior to addition of 5 nM NRG1β1. After 10 min of NRG1β1 stimulation, cells were rinsed twice with ice-cold PBS containing 1 mM sodium orthovanadate and lysed for 20 min on ice with 500 μl of cold extraction buffer (20 mM Tris-HCl (pH 7.4), 150 mM NaCl, 5 mM EDTA, 2 mM EGTA, 1 mM $ZnCl_2$, 10% glycerol, and 1% Triton X-100 supplemented just prior to use with 50 mM NaF, 1 mM sodium orthovanadate, 1 mM phenylmethylsulfonyl fluoride, and a mixture of protease inhibitors (Roche Applied Science)). For immunoprecipitations to be assayed for PI3K activity, cells were lysed with 500 μl of cold lysis buffer (25 mM Hepes (pH 8), 150 mM NaCl, 1% Nonidet P-40, 5 mM EDTA, 2 mM EGTA, 1 mM $ZnCl_2$, and 10% glycerol supplemented just prior to use with 50 mM NaF, 1 mM sodium orthovanadate, 1 mM phenylmethylsulfonyl fluoride, and the mixture of protease inhibitors) (45). Lysates were collected with a cell scraper, placed in microcentrifuge tubes, rocked at 4 °C for 10 min, and spun at 4 °C for 20 min at 11,000 × *g* to discard cell debris. Protein concentration was determined using the BCA kit for protein determination, and lysates (1.5–2 mg) were diluted to equal concentrations using extraction buffer (1 mg/ml). Agarose-conjugated protein A beads (50 μl; Santa Cruz Biotechnology) pre-washed three times with extraction buffer were preincubated for 45 min with primary antibody (1 μg/mg of protein), and lysates were added and incubated overnight with constant rotation at 4 °C. As a control, representative samples (NRG1β1-treated or not) were incubated with protein A beads without primary antibody. The next day, immunoprecipitates were spun at 4 °C for 1 min at 900 × *g* and rinsed four times with ice-cold extraction buffer. To release immunoprecipitates from the beads, 2× sample buffer (62.5 mM Tris (pH 6.8), 4% SDS, 480 mM 2-mercaptoethanol, and 40% glycerol) was added, and the proteins were denatured at 100 °C for 5 min. Proteins were resolved by 8% SDS-PAGE, transferred to a Hybond™ C Extra membrane (Amersham Biosciences) following the manufacturer's instruction, and blocked for 1 h at 37 °C in 1× TBST (150 mM NaCl, 10 mM Tris-HCl (pH 7.4), and 0.1% Tween) plus 5% nonfat milk. The membranes were incubated overnight at 4 °C in primary antibodies diluted 1:500 in TBST plus 1% nonfat milk. The next day, they were rinsed four times with TBST for 5 min each at room temperature and incubated for 1 h at room temperature with horseradish peroxidase-linked anti-rabbit (1:3000) or anti-mouse (1:10,000) secondary antibody (diluted in TBST plus 1% nonfat milk). Membranes were rinsed four times with TBST for 5 min each at room temperature, and specific binding was detected by the enhanced chemiluminescence ECL system (Amersham Biosciences) using Hyperfilm™ (Amersham Biosciences). In some cases, the membrane was stripped for 30 min at 50 °C in 0.05 M phosphate buffer (pH 6.5), 10 M urea, and 0.1 M 2-mercaptoethanol, blocked, tested with secondary antibody to verify accurate cleaning, and reprobed with the indicated primary antibodies for further analysis. The molecular masses of proteins were estimated relative to the electrophoretic mobility of cotransferred prestained molecular mass markers (Invitrogen and Bio-Rad).

Total Protein Extraction—Total proteins were extracted by lysing cells with extraction buffer as described above or by solubilizing cells in boiling Laemmli buffer (2.5% SDS and 0.125 M Tris-HCl (pH 6.8)), followed by 5 min of denaturation at 100 °C in 240 mM 2-mercaptoethanol and 18% glycerol. Protein concentration was determined by the BCA method, and equal amounts of proteins were loaded onto each lane, separated by SDS-PAGE, transferred to a Hybond™ C Extra membrane, and analyzed as described above. Bands were quantified by densitometry using the Gel Doc image documentation system (Bio-Rad) with Quantity One software. Conclusions were drawn after experiments were repeated a minimum of three times.

PI3K Assays—PI3K activity was assayed in the ErbB4 immunoprecipitates in the presence of [γ-^{32}P]ATP (Amersham Biosciences) and phosphoinositides (Sigma) as described previously (45, 46).

Motility Assay—The wound healing motility assay was used to measure two-dimensional movement. Cells were grown to confluence in 12-well plates and serum-starved for 24 h, and then a cross-shaped

wound was made on the monolayers using a sterile 200-μl pipette tip. The cells were rinsed three times with PBS and placed in serum-free DMEM with or without 5 nM NRG1β1. To obtain good reproducibility, in all experiments, the left arm of the cross was photographed. Photos were taken at the initiation of the experiment ($t = 0$) and 24 h later ($t = 24$ h) using an Olympus IX50 inverted microscope equipped with a Cool SNAP-Pro CCD camera (Media Cybernetics, Silver Spring, MD); images were edited with Image Pro-Plus software (Media Cybernetics). The areas were measured using the measurement program included. The two-dimensional movement of the cells was quantified by measuring the surface area of the wound at $t = 0$ and comparing it with the surface area at $t = 24$ h: healing percentage = $(1 - t_{24}/t_0) \times 100$.

Migration Assay—The Transwell migration assay was used to measure three-dimensional movement. Cells (10^5) resuspended in 200 μl of DMEM containing 2% FBS were seeded in the upper chamber of a Transwell (cell culture insert, no. 353097, BD Biosciences) on a porous transparent polyethylene terephthalate membrane (8.0-μm pore size, 1×10^5 pores/cm^2). The lower chamber (a 24-well plate well) was filled with DMEM containing 2% FBS with or without 5 nM recombinant NRG1β1. The 24-well plates containing cell culture inserts were incubated at 33 °C in a 5% CO_2 atmosphere saturated with H_2O. After 18 h of incubation, cells attached to the upper side of the membrane were mechanically removed using a cotton-tipped applicator. Cells that migrated to the lower side of the membrane were rinsed with PBS, fixed with 2% glutaraldehyde in PBS for 15 min at room temperature, washed five times with water, stained with 0.1% crystal violet and 20% methanol for 20 min at room temperature, washed five times with water, air-dried, and photographed using an Olympus IX50 inverted microscope equipped with a Cool SNAP-Pro CCD camera; images were edited with Image Pro-Plus software. Migrated cells (2 mm^2 of microscopic field/sample) were counted using the enclosed measurement program. Inhibitors (LY294002, U73122, or the same concentration of dimethyl sulfoxide as a control) were added to both the upper and lower chambers 30 min prior to addition of NRG1β1. In each case, the final concentration represented a 1:200 dilution of stock solutions in Me_2SO, and control cultures were treated with Me_2SO at a 1:200 dilution. We ruled out the possibility that the effect of migration inhibition was due to decreased viability caused by inhibitor toxicity by treating 1×10^5 cells (plated in a 24-well plate) for 18 h with the same amounts of inhibitors used for migration assays.

Statistical Analysis—Results from different experiments (performed at least three times in duplicate) were averaged and expressed as means ± S.D. One-way analysis of variance was used to compare data as indicated in the figure legends. Data were graphed using Microsoft Excel.

RESULTS

ErbB Expression Patterns in ST14A Cells—Previous data (13) describe functional studies on chemotaxis mediated by ErbB4 following stable expression of two isoforms (cyt1/cyt2) of this receptor in fibroblasts (NIH3T3) that endogenously express only moderate levels of the ErbB2 receptor (47). Being interested in the mechanisms by which ErbB4 intervenes in neural cell migration, we expressed the ErbB4 cDNAs in neural progenitor cells previously derived and conditionally immortalized from embryonic striatum (34). We verified in these cells the expression of ErbB1, ErbB2, and ErbB3 and the absence of ErbB4 by RT-PCR (data not shown) and Western blotting (Fig. 1). The three bands corresponding to apparent molecular masses of 80, 60, and 50 kDa are nonspecific, being recognized by anti-ErbB4 primary antibody in whole cell protein extracts from ST14A cells, which do not express ErbB4, as assessed by RT-PCR performed on parent ST14A cells (data not shown) or ST14A cells transfected with the pIRESpuro2 vector alone (see Fig. 3*B*, *vector lane*).

Expression of the Four ErbB4 Isoforms in ST14A Cells—The cDNAs corresponding to the various ErbB4 isoforms produced by alternative splicing, JMa-cyt1, JMa-cyt2, JMb-cyt1, and JMb-cyt2 (clones a1, a2, b1, and b2, respectively) (Fig. 2), were obtained by RT-PCR performed on rat olfactory bulb RNA, sequenced, and subcloned into the pIRESpuro2 vector, an internal ribosome entry site-containing vector for bicistronic expression of ErbB4 and puromycin resistance (see "Experimental Procedures"). ST14A cells were stably transfected with the expression vector incorporating the cDNAs corresponding to the four ErbB4 isoforms and with the parent vector as a control. Several puromycin-resistant subclones were isolated, and the presence of exogenous protein was confirmed by Western blot analysis (data not shown). For further analysis, two positive clones for each isoform and one control were selected (Fig. 3*A*). To investigate for possible transcriptional *trans*-regulation between different ErbB4 isoforms, each positive clone was analyzed by RT-PCR to detect the known alternative splicing isoforms (Fig. 3*B*). Our data show that each subclone expressed only the isoform we transfected, ruling out *trans*-regulation events.

Transfected cells do not show significant morphology variations. To better characterize the different ErbB4-expressing clones, growth rate analysis was performed in low serum for comparison in the presence and absence of NRG1β1 (data not shown). At $t = 18$ h, the time used for motility and migration assays, we did not observe significant differences between different clones and between treated and untreated cells; however, comparing all clones at $t_2 = 48$ h and $t_4 = 96$ h, we observed that they can be divided into two groups: a lower rate group, including wild-type ST14A cells and cells expressing

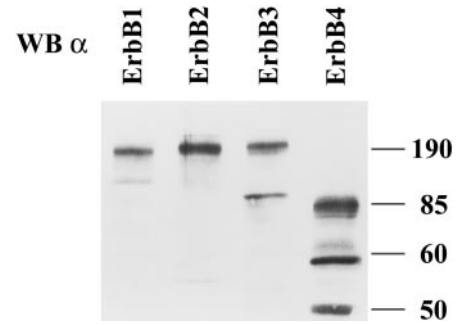

FIG. 1. **Wild-type ST14A cells express ErbB1, ErbB2, and ErbB3, but not ErbB4.** Whole cell protein extracts (50 μg) from wild-type (parent) ST14A cells were analyzed by Western blotting (*WB*) and ECL for ErbB1 (*first lane*), ErbB2 (*second lane*), ErbB3 (*third lane*), and ErbB4 (*fourth lane*) expression. The three bands (*fourth lane*) corresponding to apparent molecular masses of 80, 60, and 50 kDa are nonspecific, being recognized by anti-ErbB4 primary antibody in whole cell protein extracts from cells not expressing ErbB4. The molecular mass standards are expressed in kilodaltons.

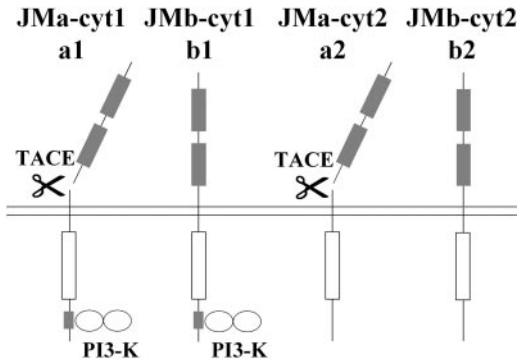

FIG. 2. **Schematic presentation of the four ErbB4 isoforms.** Two pairs of naturally occurring ErbB4 isoforms differing in their juxtamembrane (JMa/JMb) and C termini (cyt1/cyt2) have been described: JMa-cyt1, JMb-cyt1, JMa-cyt2, and JMb-cyt2 (clones a1, b1, a2, and b2, respectively). One isoform pair is characterized by alternative splicing of exons located in the extracellular juxtamembrane region, conferring (JMa) or not (JMb) susceptibility to proteolytic cleavage operated by a member of the metalloprotease-disintegrin family (ADAM), the tumor necrosis factor-α-converting enzyme (*TACE*) (7). The other ErbB4 isoform pair is characterized by the presence (cyt1) or absence (cyt2) of a cytoplasmic exon containing a docking site for PI3K by Junttila *et al.* (4), modified.

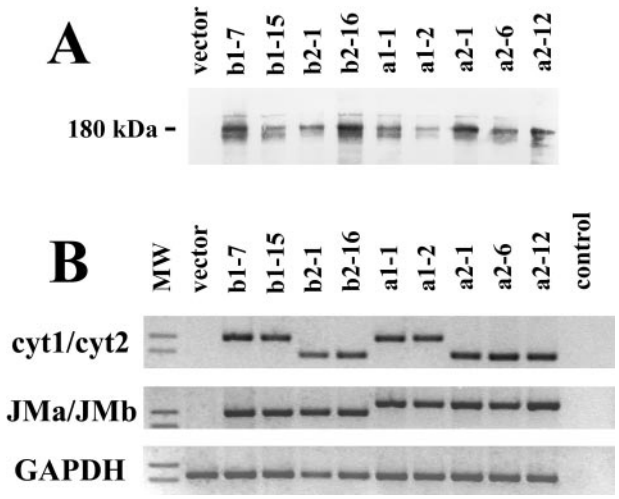

FIG. 3. **Stable transfected clones express ErbB4.** *A*, whole cell protein extracts (50 μg) from ST14A cells stably transfected with the pIRESpuro2 vector alone or expressing each ErbB4 isoform (JMa-cyt1 = clone a1, JMa-cyt2 = clone a2, JMb-cyt1 = clone b1, and JMb-cyt2 = clone b2; see Fig. 2) were analyzed by Western blotting and ECL for ErbB4 expression levels. *B*, the same clones were analyzed by RT-PCR for ErbB4 and GAPDH as a control using specific primers designed to detect the cyt1/cyt2 and JMa/JMb isoforms. The *MW lane* contains the molecular size standards (BenchTop pGEM DNA markers). The bands shown correspond to 222 and 179 bp. The predicted amplicon molecular sizes are as follows: cyt1, 213 bp; cyt2, 165 bp; JMa, 246 bp; JMb, 207 bp; and GAPDH, 188 bp.

ErbB4 JMb-cyt1 isoforms (b1-7 and b1-15), and a higher rate group, including the remaining three isoforms.

NRG1β1 Activates the ErbB4 Receptor—To establish whether the different isoforms can be activated by treatment with exogenous NRG1β1, we performed immunoprecipitation experiments. Proteins from whole cell lysates of selected serum-starved clones treated or not with recombinant NRG1β1 were immunoprecipitated using anti-ErbB4 antibody. The immunoprecipitates were separated by SDS-PAGE, transferred to membranes, and probed for phosphotyrosines (Fig. 4*B*); after stripping, the membranes were reprobed for ErbB4 (Fig. 4*A*). Bands of phosphoproteins at the appropriate molecular masses were detected: an ~180-kDa band (present in all the isoforms) corresponding to the entire receptor and an ~80-kDa band (present only in the JMa isoforms) derived by proteolytic cleavage attributable to tumor necrosis factor-α-converting enzyme, a member of the transmembrane ADAM protease family, also designated ADAM17 (7), which recognizes the JMa isoform, but not the JMb isoform. Shedding activity releases the ErbB4 ectodomain fragment into the medium and leaves an ~80-kDa fragment, representing the transmembrane and cytoplasmic domains associated with the cell (48), which is an active tyrosine kinase at least *in vitro* (8). In the b1-7 clone, we observed an unusual ~90-kDa band that did not correspond to the known proteolytic intracellular fragment and, moreover, did not seem to be tyrosine-phosphorylated. Our data show that the amount of phosphorylated ErbB4 (~180 kDa) increased when the receptors were stimulated by NRG1β1, exhibiting different intensities among clones, being higher for clones b1, b2, and a2 and lower for clone a1.

PI3K Co-immunoprecipitates with All ErbB4 Isoforms—After a further stripping, the membranes were reprobed for the p85 subunit of PI3K (Fig. 4*C*). Interestingly, our results show that the amount of PI3K associating with ErbB4 increased when the receptors were stimulated by NRG1β1 and, intriguingly, that all the ErbB4 isoforms co-immunoprecipitated with PI3K. Such interaction with PI3K has been described downstream from NRG1β in NIH3T3 cells transfected with ErbB4 cyt1, but not in NIH3T3 transfected with ErbB4 cyt2 (13). The two isoforms differ by 16 amino acids present only in the cytoplasmic tail of ErbB4 cyt1, including a sequence that matches the consensus binding sequence for the p85 subunit of PI3K (49). NIH3T3 cells analyzed by Kainulainen *et al.* (13) expressed one transfected ErbB4 isoform (a1 or a2) and moderate levels of endogenous ErbB2 (47), but not ErbB1 and ErbB3. In contrast, ST14A cells transfected with one of the four ErbB4 isoforms (a1, a2, b1, or b2) expressed not only ErbB2, but also the EGF receptor and ErbB3. ErbB3 is the only member of the ErbB family that incorporates multiple PI3K-binding sites and has been shown to be a major recruiter of PI3K (50–52). Each of the six *YXXM* motifs has the potential to individually bind the PI3K holoenzyme, albeit to a significantly lower extent than the six *YXXM* motifs together (44).

As a consequence of NRG1β1-induced heterodimerization with ErbB4, ErbB3 could account for ErbB4 cyt2 and PI3K co-immunoprecipitation. To test this hypothesis, we transiently expressed, in COS-7 cells endogenously expressing ErbB2, but not ErbB3 (44), ErbB4 JMb-cyt1 or JMb-cyt2 together with wild-type ErbB3 or ErbB3-6F, a mutant ErbB3 protein unable to bind PI3K (44), or the parent vector as a control and examined the ability of these receptors to associate with PI3K upon stimulation by NRG1β1. Immunoprecipitation analysis confirmed that, whereas ErbB4 cyt1 could bind PI3K independently of ErbB3, ErbB4 cyt2 needed wild-type ErbB3 to co-immunoprecipitate with PI3K (Fig. 5).

All ErbB4 Isoforms Activate PI3K and Akt—By co-immunoprecipitation analysis, we demonstrated that ErbB4 recruits PI3K upon NRG1β1 stimulation. To prove PI3K activation, as a preliminary test, PI3K activity was analyzed in ErbB4 immunoprecipitates by *in vitro* kinase assays in which the phosphatidylinositol 3-phosphate product was resolved by thin layer chromatography (data not shown). PI3K activity co-immunoprecipitated with both the ErbB4 cyt1 and cyt2 isoforms, although with lower intensity with the cyt2 isoform.

Phosphorylation of Akt provides an excellent indication of PI3K activation in the cell; phosphorylation at Thr^{308} and Ser^{473} is critical for activation of the protein Ser/Thr kinase activity of Akt (53). Therefore, to confirm PI3K activation, we investigated Akt phosphorylation at Ser^{473} in ST14A cells expressing either the ErbB4 cyt1 isoform (clones b1-15 and a1-2) or the ErbB4 cyt2 isoform (clones b2-16 and a2-6) following NRG1β1 stimulation (Fig. 6). We observed a very strong NRG1β1-dependent increase in phosphorylation of Akt at Ser^{473} in cells expressing ErbB4 cyt1 and cyt2. The very slight phosphorylation observed in control cells (vector) could be the consequence of ErbB2-ErbB3 heterodimer activation (44) and demonstrates that the strong phosphorylation observed in our samples can be ascribed to ErbB4 activation.

Two-dimensional Motility Assay—Finally, being interested in studying migration mediated by ErbB4, we performed a first round of experiments to determine whether NRG1β1 treatment can modulate motility, defined here as two-dimensional movement or chemokinesis. We selected as a model the wound healing assay, in which the repopulation of cells in a cell-free region (wound) can be examined quantitatively. Stable ErbB4 clones and control cells were grown until they progressively reached confluence and then serum-starved for 24 h. A cross-shaped wound was created in the monolayers, and cells were placed in medium with or without NRG1β1 and photographed. Twenty-four hours later, the cross-shaped wound was photographed in the same region, and the healing percentage was quantified comparing the wound area at $t = 0$ and $t = 24$ h. Fig. 7 (*upper*) shows representative digital images of the wounded region before and after the incubation period; the healing per-

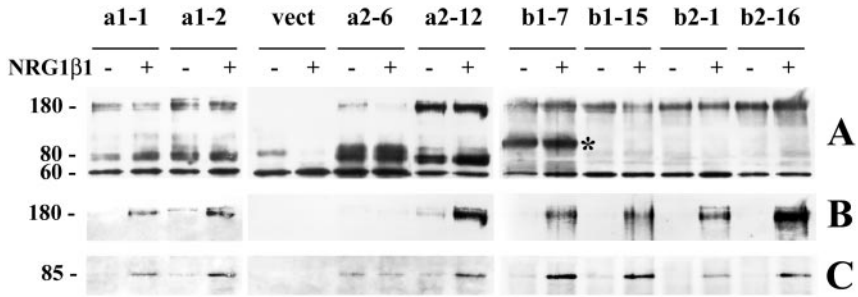

FIG. 4. **NRG1β1 induces phosphorylation of ErbB4 proteins and PI3K recruitment.** Representative clones expressing the four ErbB4 isoforms (JMa-cyt1 = clone a1, JMa-cyt2 = clone a2, JMb-cyt1 = clone b1, and JMb-cyt2 = clone b2; see Fig. 2) and a control clone transfected with the pIRESpuro2 vector (*vect*) alone were starved for 24 h in the absence of serum, pretreated for 30 min with 1 mM sodium orthovanadate, and stimulated (+) or not (−) with 5 nM NRG1β1 for 10 min at 33 °C. Whole cell lysates (1.7 mg) were immunoprecipitated with anti-ErbB4 antibody and analyzed using anti-ErbB4 antibody (*A*), anti-phosphotyrosine antibody (*B*), and anti-PI3K p85 subunit antibody (*C*). In all samples (including the control clone), anti-ErbB4 antibody recognized a nonspecific band of ~60 kDa. In all ErbB4-expressing clones, an ~180-kDa band corresponding to the full-length ErbB4 receptor was bound by anti-ErbB4 antibody and, following ligand stimulation, by anti-phosphotyrosine antibody. The ~80-kDa cytoplasmic fragment recognized by anti-ErbB4 antibody was present, as expected, only in JMa-expressing clones (a1 and a2). A nonspecific ~90-kDa band (*) was present only in clone b1-7, but it was not phosphorylated at tyrosine (not shown). (For clone a2-6, the untreated sample contained more protein than the treated sample as assessed by the anti-ErbB4 immunoblotting shown in *A*).

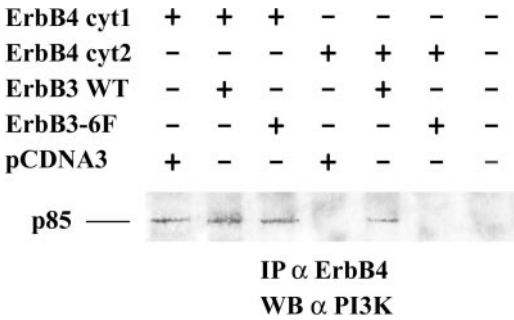

FIG. 5. **ErbB4 cyt2 needs wild-type ErbB3 to associate with PI3K.** COS-7 cells were transiently cotransfected with the pIRESpuro2 vector incorporating the ErbB4 cyt1 or cyt2 isoform and with either the parent expression vector (pcDNA3) or the vector incorporating wild-type (*WT*) ErbB3 or ErbB3-6F cDNA as indicated. Transiently transfected cells (serum-starved for 24 h) were treated for 10 min at 37 °C in the presence of 5 nM NRG1β1 and subjected to detergent lysis; cell lysates were immunoprecipitated (*IP*) with anti-ErbB4 antibody and immunoblotted with antibody recognizing the p85 subunit of PI3K. *WB*, Western blot.

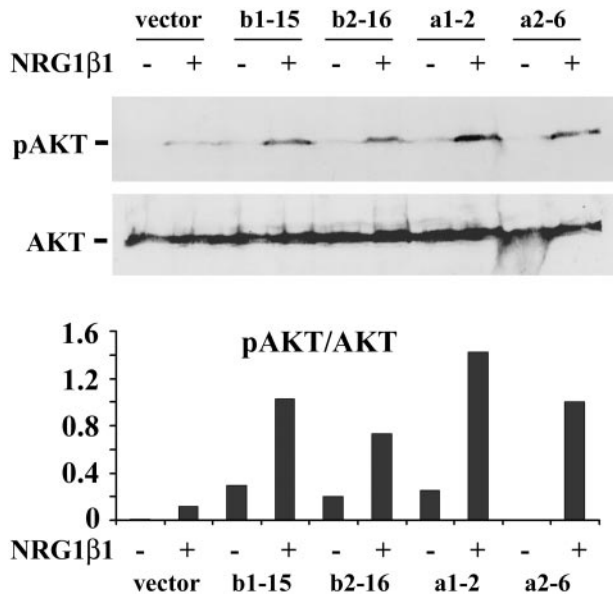

FIG. 6. **NRG1β1 induces Akt phosphorylation in ErbB4-expressing cells.** *Upper*, the ability of NRG1β1 to induce phosphorylation of Akt at Ser^{473} in ST14A cells stably expressing ErbB4 cyt1 (clones b1-15 and a1-2) or ErbB4 cyt2 (clones b2-16 and a2-6) or transfected with the pIRESpuro2 parent vector was analyzed via immunoblotting. Cells starved for 24 h were stimulated for 10 min at 33 °C in the presence (+) or absence (−) of 5 nM NRG1β1 and lysed in boiling Laemmli buffer. Whole cell lysates were immunoblotted with anti-phospho-Ser^{473} Akt antibody (*pAKT*) and, after membrane stripping, with anti-total Akt antibody (*AKT*). *Lower*, the results from quantitative densitometric analysis show, for each sample, the ratio between phospho-Akt and total Akt.

centage was quantified and is displayed graphically (Fig. 7, *lower*). Our results show that NRG1β1 treatment induced a statistically significant motility increase only in clones expressing ErbB4 JMb-cyt1 and JMb-cyt2. We suppose that the wound (and the consequent absence of contact inhibition) stimulates motility and proliferation so strongly that the differences between clones and between treated and untreated samples cannot be appreciated significantly. Only clone a2-6 showed a significant increase in motility compared with control cells; however, it displayed high basal activity observed also in the Transwell assays discussed below.

ErbB4 Activation Stimulates Cell Invasion in Three-dimensional Migration Assays—To evaluate the ability of stable transfectants to migrate in a three-dimensional environment, hence more similar to brain tissues, we assayed Transwell migration. A preliminary experiment was carried out with clone b2-16 using NRG1β1 at 10 pM to 10 nM. Cells were plated in the upper chamber of a Transwell filter and allowed to migrate for 18 h in response to NRG1β1 added to the lower chamber before being fixed, stained, and counted. Fig. 8 shows that the number of migrating cells was augmented significantly in the presence of increasing amounts of NRG1β1 from 1 nM, with a peak at 5 nM.

Representative clones for each ErbB4 isoform and a negative control (cells transfected with empty vector) were plated in the upper chamber of a Transwell filter and allowed to migrate for 18 h with or without 5 nM NRG1β1 added to the lower chamber. Fig. 9 shows that, for each ErbB4 isoform, NRG1β1 treatment significantly increased the number of cells that migrated through the filter for each treated clone compared with the respective untreated clone and with the treated negative control (empty vector).

ErbB4-mediated Migration Requires PI3K (but Not Phospholipase Cγ) Activity—Data highlighting the need for PI3K in ErbB4 (cyt1 isoform)-mediated migration (13) and our results concerning ErbB4 and PI3K co-immunoprecipitation prompted us to investigate a possible role of this signal transduction protein in cell migration. We performed Transwell assays in the presence of 5 nM NRG1β1 and increasing amounts of the PI3K inhibitor LY294002 (1–100 μM) (Fig. 10). To exclude a

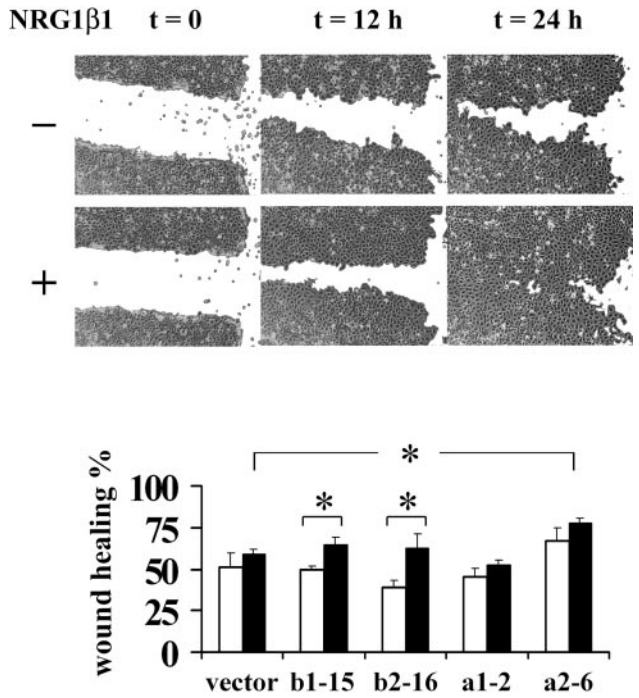

FIG. 7. **Motility of ErbB4-expressing cells.** A cross-shaped wound was made on serum-starved confluent monolayers of cell clones representative of each ErbB4 isoform and the control vector. The cells were rinsed and placed in medium with (+) or without (−) 5 nM NRG1β1. *Upper*, images were taken at the start of the experiment ($t = 0$) and 12 and 24 h later. Clone b1-15 was chosen as a representative. Wound healing was evaluated as the decrease in the surface area of the wound at $t = 24$ h. *Lower*, the percent wound healing was quantified and is displayed, where healing percentage = $(1 - t_{24}/t_0) \times 100$. *Bars* represent means ± S.D. Experiments were performed three times in duplicate. *, $p < 0.05$.

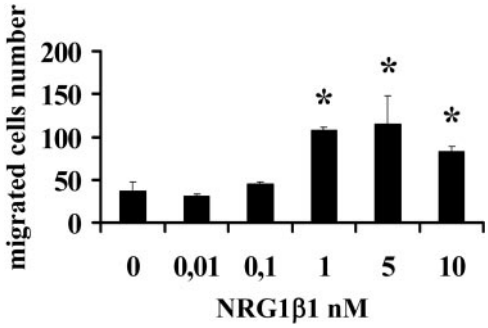

FIG. 8. **NRG1β1 stimulates migration of ErbB4-expressing cells.** The ability of NRG1β1 to stimulate chemotaxis of a representative clone expressing ErbB4 (b2-16) was analyzed by Transwell migration assay. Cells (10^5) were plated in the upper chamber of a Transwell filter and allowed to migrate for 18 h in response to NRG1β1 added to the lower chamber (using NRG1β1 at 10 pM to 10 nM, corresponding to 0.1–100 ng/ml) before being fixed and stained. Cells (2 mm^2 of microscopic field/sample) were photographed, and migrated cells were counted. Data represent means ± S.D. *, $p < 0.05$ (stimulated samples compared with the untreated sample).

vehicle inhibitory effect, all samples received the same final concentration of dimethyl sulfoxide. Our data show that, in ErbB4-expressing cells, increasing amounts of the PI3K inhibitor resulted in greater reduction in NRG1β1-induced migration. In contrast, when we performed Transwell assays in the presence of 5 nM NRG1β1 and increasing amounts of the phospholipase Cγ inhibitor U73122 (0.1–5 μM) (data not shown), we did not observe a significant decrease in NRG1β1-induced migration.

DISCUSSION

This is the first work demonstrating that, in immortalized neural progenitor cells, ErbB4 expression is necessary to mediate NRG1β1-induced migration and that this phenomenon occurs via a PI3K-mediated mechanism. We began our research prompted by several intriguing studies suggesting that ErbB4 may be involved in cell migration and, specially, in neural cell migration. In fact, interneurons tangentially migrating from the ganglionic eminences express ErbB4 (29). When the glial ErbB4 receptor is blocked, neurons fail to induce radial glial formation, and their migration along radial glial fibers is impaired (33). ErbB4 knockout mice (genetically rescued from embryonic lethality) display defects in cranial neural crest migration and increased numbers of large interneurons within the cerebellum (32).

In our laboratory, long-distance migration and differentiation of neuronal precursors in adult mammalian brain have been extensively investigated in the paradigm represented by the subependymal layer-olfactory bulb system (reviewed in Ref. 54). The olfactory bulb, together with the dentate gyrus of the hippocampus, belongs to those few specific regions of the brain undergoing constant neurogenesis during adulthood (55). Newly formed cells of the olfactory bulb are generated from multipotent stem cells that reside in the subependymal layer of the lateral ventricles (see Ref. 56 for a review). The progeny of these stem cells undergo long-distance tangential migration along the rostral extension (rostral migratory stream) of the subependymal layer, reaching the main (57) and accessory (58) olfactory bulb, where they differentiate into the two principal classes of interneurons, the granule and periglomerular cells. Intriguingly, cells coming out of the rostral migratory stream of the subependymal layer, as well as isolated cells in the granule cell layer, possibly migrating cells, strongly express ErbB4, and ErbB4 immunoreactivity is found in all the periglomerular and mitral/tufted cells of the olfactory bulb (26, 28).

Many efforts have been made to solve the ErbB1 signal transduction mechanism, whereas little is known about ErbB4 receptor signaling. Neuregulin-stimulated ErbB4 receptor (cyt1 isoform) has been shown to interact with the adaptor protein Shc (Src homology and collagen domain) and with the p85 subunit of PI3K (59). In addition, it has been demonstrated that, in NIH3T3 cells overexpressing ErbB4 (cyt1 isoform), HB-EGF induces association of PI3K activity with ErbB4 and is a potent chemotactic factor (60). Moreover, chemotaxis is inhibited by wortmannin, a PI3K inhibitor, suggesting a possible role for PI3K in mediating HB-EGF-stimulated chemotaxis.

A number of studies in several types of cell lines (reviewed in Ref. 61) showed that, in response to external stimuli, PI3K activates protein kinase B/Akt, which phosphorylates Raf-1 at Ser^{259}, inhibiting Raf-1 and the subsequent extracellular signal-regulated kinase activity (62, 63). This pathway has been recently confirmed for neuregulin-induced ErbB4 signal transduction (64).

Previous studies suggest that neuregulin (and other growth factors)-activated PI3K may be involved in actin reorganization, formation of lamellipodia, membrane ruffling, and cell migration (65–68). PI3K cooperates with the small GTPases Rac and Cdc42 and with p21-activated kinase-1 in the formation of actin-rich extensions via stimulation of actin polymerization (66, 69–71). There is also evidence for the association of PI3K with microtubules (72) and for the involvement of the microtubule system in the outgrowth of cell processes induced by PI3K (73, 74).

The aim of our research was to study the role of ErbB4 in neural cell migration. We began our analysis by seeking a

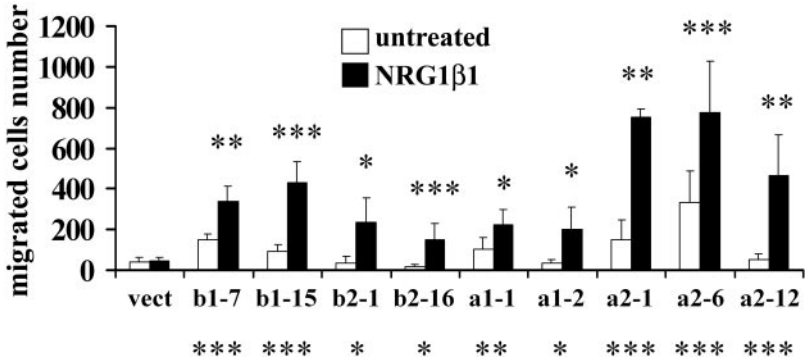

FIG. 9. **ErbB4 is necessary to mediate NRG1β1-induced migration, and each ErbB4 isoform significantly mediates this activity.** Representative clones expressing the four ErbB4 isoforms (JMa-cyt1 = clone a1, JMa-cyt2 = clone a2, JMb-cyt1 = clone b1, and JMb-cyt2 = clone b2; see Fig. 2) and a control clone transfected with the pIRESpuro2 vector (*vect*) alone were assayed for Transwell migration. Cells (10^5) were plated in the upper chamber of a Transwell filter and allowed to migrate for 18 h in the presence (*black bars*) or absence (untreated; *white bars*) of 5 nM NRG1β1 added to the lower chamber before being fixed and stained. Cells (2 mm^2 of microscopic field/sample) were photographed, and migrated cells were counted. Data represent means ± S.D. from several independent assays. *, $p < 0.05$; **, $p < 0.01$; ***, $p < 0.001$ (*upper asterisks*, for each clone, treated samples compared with untreated samples; *lower asterisks*, for each clone, NRG1β1-treated samples compared with the NRG1β1-treated vector, showing that data for all samples are significant, suggesting that the presence of ErbB4 is necessary to mediate NRG1β1-induced migration).

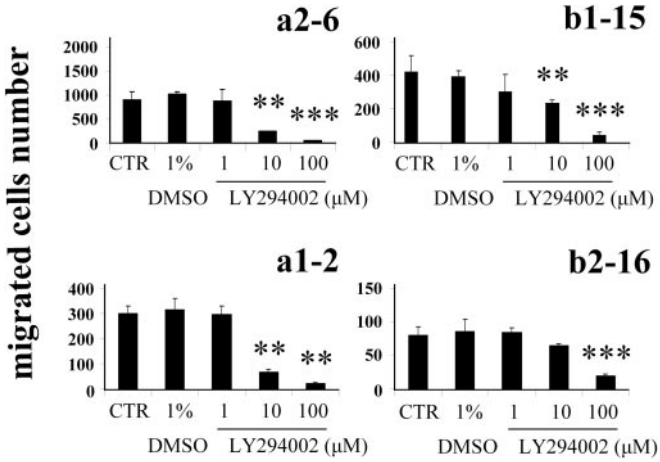

FIG. 10. **PI3K inhibition decreases NRG1β1-induced migration.** Representative clones expressing the four ErbB4 isoforms (JMa-cyt1 = clone a1, JMa-cyt2 = clone a2, JMb-cyt1 = clone b1, and JMb-cyt2 = clone b2; see Fig. 2) were assayed for Transwell migration in the presence, in both the upper and lower chambers, of increasing amounts of the PI3K inhibitor LY294002 dissolved in dimethyl sulfoxide (*DMSO*) added 30 min prior to stimulation with 5 nM NRG1β1. All samples, except the control (*CTR*), had the same final concentration of dimethyl sulfoxide. All samples were stimulated with 5 nM NRG1β1. Data represent means ± S.D. **, $p < 0.01$; ***, $p < 0.001$ (control and LY294002 inhibitor-treated samples compared with the untreated sample (1% Me_2SO)).

suitable *in vitro* model, and we identified an embryonic neuroepithelial striatal immortalized cell line, ST14A (34), which lacks ErbB4, but expresses all other members of the ErbB family. Starting from data describing two different isoform pairs (5, 13), we cloned the full-length cDNAs encoding the four potential ErbB4 isoforms (4) and expressed them in our cell model. We found that NRG1β1 induced ErbB4 phosphorylation and co-immunoprecipitation of PI3K with all ErbB4 isoforms. In addition, we demonstrated that, following NRG1β1 stimulation, all ErbB4 isoforms activated PI3K and induced Akt phosphorylation at Ser^{473}, which provides an excellent indication of PI3K activation in the cell (53).

However, according to a previous study (13), only the ErbB4 cyt1 isoform should interact with PI3K because the cyt2 isoform lacks the consensus sequence (49) for the binding of this signal transduction protein. Nevertheless, the previous model is different: fibroblasts expressing moderate levels of ErbB2 (47) and stably transfected with an ErbB4 isoform were studied, whereas we studied a neural progenitor cell line endogenously expressing ErbB1, ErbB2, and ErbB3 and one transfected ErbB4 isoform. Therefore, in NIH3T3 fibroblasts, ErbB4 can homodimerize or heterodimerize only with ErbB2. ErbB2 has been described to associate with Src (75, 76), a potential mediator of PI3K activation (77). Nevertheless, in NIH3T3 cells, it has been shown that cyt2, the ErbB4 isoform that does not activate PI3K, mediates proliferation, but not survival and chemotaxis (13), which are mediated by PI3K, suggesting that ErbB2 cannot account for the PI3K recruitment mediated by NRG1β1-stimulated ErbB4.

Intriguingly, there are six PI3K-binding motifs in the C-terminal domain of ErbB3 (50–52), and one simple explanation may include direct recruitment of PI3K by the activated ErbB3 receptor. We tested this hypothesis by expressing ErbB4 cyt2 together with wild-type ErbB3 (43) or ErbB3 mutated at the six tyrosines included in the PI3K-binding motifs (44), and we demonstrated that the ErbB4 cyt2 isoform could co-immunoprecipitate with PI3K only when coexpressed with the wild-type ErbB3 receptor.

Finally, to test our preliminary hypothesis, we performed migration assays and showed that ErbB4 confers to ST14A cells the ability to respond to NRG1β1 through migration. This ligand is not ErbB4-specific and could activate the ErbB3 receptor; nevertheless, control cells expressing ErbB3, but lacking ErbB4, failed to migrate, indicating that, in our cell model, ErbB4 is necessary for this activity. Our data show that every ErbB4 isoform (endowed or not with the PI3K-binding motif) mediates NRG1β1-induced migration, although with different intensity, and we have demonstrated that PI3K activation is necessary for ErbB4-mediated migration either directly or indirectly through ErbB3 heterodimerization.

Acknowledgments—We thank Dr. John G. Koland for the generous gift of the ErbB3 and ErbB3-6F mammalian expression vectors. We gratefully acknowledge Dr. Andrea Graziani for fruitful discussions, Drs. Daniela Gramaglia and Andrea Rasola for helpful suggestions, and Dr. Tiziana Merlo for technical assistance.

REFERENCES

1. Olayioye, M. A., Neve, R. M., Lane, H. A., and Hynes, N. E. (2000) *EMBO J.* **19,** 3159–3167
2. Guy, P. M., Platko, J. V., Cantley, L. C., Cerione, R. A., and Carraway, K. L., III (1994) *Proc. Natl. Acad. Sci. U. S. A.* **91,** 8132–8136
3. Carpenter, G. (2003) *Exp. Cell Res.* **284,** 66–77
4. Junttila, T. T., Sundvall, M., Maatta, J. A., and Elenius, K. (2000) *Trends Cardiovasc. Med.* **10,** 304–310
5. Elenius, K., Corfas, G., Paul, S., Choi, C. J., Rio, C., Plowman, G. D., and Klagsbrun, M. (1997) *J. Biol. Chem.* **272,** 26761–26768
6. Cheng, Q.-C., Tikhomirov, O., Zhou, W., and Carpenter, G. (2003) *J. Biol.*

Chem. **278,** 38421–38427
7. Rio, C., Buxbaum, J. D., Peschon, J. J., and Corfas, G. (2000) *J. Biol. Chem.* **275,** 10379–10387
8. Vecchi, M., and Carpenter, G. (1997) *J. Cell Biol.* **139,** 995–1003
9. Ni, C.-Y., Murphy, M. P., Golde, T. E., and Carpenter, G. (2001) *Science* **294,** 2179–2181
10. Lee, H.-J., Jung, K.-M., Huang, Y. A., Bennet, L. B., Lee, J. S., Mei, L., and Kim, T.-W. (2002) *J. Biol. Chem.* **277,** 6318–6323
11. Komuro, A., Nagai, M., Navin, N. E., and Sudol, M. (2003) *J. Biol. Chem.* **278,** 33334–33341
12. Omerovic, J., Puggioni, E. M., Napoletano, S., Visco, V., Fraioli, R., Frati, L., Gulino, A., and Alimandi M. (2004) *Exp. Cell Res.* **294,** 469–479E. M. R.
13. Kainulainen, V., Sundvall, M., Maatta, J. A., Santiestevan, E., Klagsbrun, M., and Elenius, K. (2000) *J. Biol. Chem.* **275,** 8641–8649
14. Falls, D. L. (2003) *Exp. Cell Res.* **284,** 14–30
15. Pinkas-Kramarski, R., Eilam, R., Spiegler, O., Lavi, S., Liu, N., Chang, D., Wen, D., Schwartz, M., and Yarden, Y. (1994) *Proc. Natl. Acad. Sci. U. S. A.* **91,** 9387–9391
16. Raabe, T. D., Clive, D. R., Wen, D., and DeVries, G. H. (1997) *J. Neurochem.* **69,** 1859–1863
17. Pollock, G. S., Franceschini, I. A., Graham, G., Marchionni, M., and Barnett, S. C. (1999) *Eur. J. Neurosci.* **11,** 769–780
18. Meyer, D., Yamaai, T., Garratt, A., Riethmacher-Sonnenberg, E., Kane, D., Theill, L. E., and Birchmeier, C. (1997) *Development* (*Camb.*) **124,** 3575–3586
19. Pinkas-Kramarski, R., Eilam, R., Alroy, I., Levkowitz, G., Lonai, P., and Yarden, Y. (1997) *Oncogene* **15,** 2803–2815
20. Steiner, H., Blum, M., Kitai, S. T., and Fedi, P. (1999) *Exp. Neurol.* **159,** 494–503
21. Gerecke, K. M., Wyss, J. M., Karavanova, I., Buonanno, A., and Carroll, S. L. (2001) *J. Comp. Neurol.* **433,** 86–100
22. Lindholm, T., Cullheim, S., Deckner, M., Carlstedt, T., and Risling, M. (2002) *Exp. Brain Res.* **142,** 81–90
23. Bermingham-McDonogh, O., McCabe, K. L., and Reh, T. A. (1996) *Development* (*Camb.*) **122,** 1427–1438
24. Lai, C., and Feng, L. (2004) *Biochem. Biophys. Res. Commun.* **314,** 535–542
25. Lai, C., and Feng, L. (2004) *Biochem. Biophys. Res. Commun.* **319,** 603–611
26. Perroteau, I., Oberto, M., Ieraci, A., Bovolin, P., and Fasolo, A. (1998) *Ann. N. Y. Acad. Sci.* **855,** 255–259
27. Oberto, M., Soncin, I., Bovolin, P., Voyron, S., De Bortoli, M., Dati, C., Fasolo, A., and Perroteau, I. (2001) *Eur. J. Neurosci.* **14,** 513–521
28. Perroteau, I., Oberto, M., Soncin, I., Voyron, S., De Bortoli, M., Bovolin, P., and Fasolo, A. (1999) *Cell. Mol. Biol.* (*Noisy-Le-Grand*) **45,** 293–301
29. Yau, H. J., Wang, H. F., Lai, C., and Liu, F. C. (2003) *Cereb. Cortex* **13,** 252–264
30. Gassmann, M., Casagranda, F., Orioli, D., Simon, H., Lai, C., Klein, R., and Lemke, G. (1995) *Nature* **378,** 390–394
31. Golding, J. P., Trainor, P., Krumlauf, R., and Gassmann, M. (2000) *Nat. Cell Biol.* **2,** 103–109
32. Tidcombe, H., Jackson-Fisher, A., Mathers, K., Stern, D. F., Gassmann, M., and Golding, J. P. (2003) *Proc. Natl. Acad. Sci. U. S. A.* **100,** 8281–8286
33. Rio, C., Rieff, H. I., Qi, P., Khurana, T. S., and Corfas, G. (1997) *Neuron* **19,** 39–50; Correction (1997) *Neuron* **19,** 1349
34. Cattaneo, E., and Conti, L. (1998) *J. Neurosci. Res.* **53,** 223–234
35. Ehrlich, M. E., Conti, L., Toselli, M., Taglietti, L., Fiorillo, E., Taglietti, V., Ivkovic, S., Guinea, B., Tranberg, A., Sipione, S., Rigamonti, D., and Cattaneo. E. (2001) *Exp. Neurol.* **167,** 215–226
36. Wainwright, M. S., Perry, B. D., Won, L. A., O'Malley, K. L., Wang, W. Y., Ehrlich, M. E., and Heller, A. (1995) *J. Neurosci.* **15,** 676–688
37. Lundberg, C., Martinez-Serrano, A., Cattaneo, E., McKay, R. D., and Bjorklund, A. (1997) *Exp. Neurol.* **145,** 342–360
38. Rigamonti, D., Bauer, J. H., De Fraja, C., Conti, L., Sipione, S., Sciorati, C., Clementi, E., Hackam, A., Hayden, M. R., Li, Y., Cooper, J. K., Ross, C. A., Govoni, S., Vincenz, C., and Cattaneo, E. (2000) *J. Neurosci.* **20,** 3705–3713
39. Zuccato, C., Ciammola, A., Rigamonti, D., Leavitt, B. R., Goffredo, D., Conti, L., MacDonald, M. E., Friedlander, R. M., Silani, V., Hayden, M. R., Timmusk, T., Sipione, S., and Cattaneo, E. (2001) *Science* **293,** 493–498
40. Zuccato, C., Tartari, M., Crotti, A., Goffredo, D., Valenza, M., Conti, L., Cataudella, T., Leavitt, B. R., Hayden, M. R., Timmusk, T., Rigamonti, D., and Cattaneo, E. (2003) *Nat. Genet.* **35,** 76–83
41. Mautino, B., Dalla Costa, L., Gambarotta, G., Perroteau, I., Fasolo, A., and Dati, C. (2004) *Protein Expression Purif.* **35,** 25–31
42. Kueng, W., Silber, E., and Eppenberger, U. (1989) *Anal. Biochem.* **182,** 16–19
43. Hellyer, N. J., Kim, H.-H., Greaves, C. H., Sierke, S. L., and Koland, J. G. (1995) *Gene* (*Amst.*) **165,** 279–284
44. Hellyer, N. J., Kim, M.-S., and Koland, J. G. (2001) *J. Biol. Chem.* **276,** 42153–42161
45. Graziani, A., Gramaglia, D., Cantley, L. C., and Comoglio, P. M. (1991) *J. Biol. Chem.* **266,** 22087–22090
46. Carpenter, C. L., Duckworth, B. C, Auger, K. R., Cohen, B., Schaffhausen, B. S., and Cantley, L. C. (1990) *J. Biol. Chem.* **265,** 19704–19711
47. Vijapurkar, U., Kim, M.-S., and Koland, J. G. (2003) *Exp. Cell Res.* **284,** 291–302
48. Vecchi, M., Baulida, J., and Carpenter, G. (1996) *J. Biol. Chem.* **271,** 18989–18995
49. Songyang, Z., Shoelson, S. E., Chaudhuri, M., Gish, G., Pawson, T., Haser, W. G., King, F., Roberts, T., Ratnofsky, S., and Lechleider, R. J. (1993) *Cell* **72,** 767–778
50. Kim, H.-H., Sierke, S. L., and Koland, J. G. (1994) *J. Biol. Chem.* **269,** 24747–24755
51. Soltoff, S. P., Carraway, K. L., III, Prigent, S. A., Gullick, W. G., and Cantley, L. C. (1994) *Mol. Cell. Biol.* **14,** 3550–3558
52. Hellyer, N. J., Cheng, K., and Koland, J. G. (1998) *Biochem. J.* **333,** 757–763
53. Alessi, D. R., Andjelkovic, M., Caudwell, B., Cron, P., Morrice, N., Cohen, P., and Hemmings, B. A. (1996) *EMBO J.* **15,** 6541–6551
54. Fasolo, A., Peretto, P., and Bonfanti, L. (2002) *Chem. Senses* **27,** 581–582
55. Gage, F. H. (2002) *J. Neurosci.* **22,** 612–613
56. Weiss, S., Reynolds, B. A., Vescovi, A. L., Morshead, C., Craig, C. G., and van der Kooy, D. (1996) *Trends Neurosci.* **19,** 387–393
57. Coskun, V., and Luskin, M. B. (2002) *J. Neurosci. Res.* **69,** 795–802
58. Bonfanti, L., Peretto, P., Merighi, A., and Fasolo, A. (1997) *Neuroscience* **81,** 489–502
59. Cohen, B. D., Green, J. M., Foy, L., and Fell, H. P. (1996) *J. Biol. Chem.* **271,** 4813–4818
60. Elenius K., Paul, S., Allison, G., Sun, J., and Klagsbrun, M. (1997) *EMBO J.* **16,** 1268–1278
61. Rameh, L. E., and Cantley, L. C. (1999) *J. Biol. Chem.* **274,** 8347–8450
62. Dhillon, A. S., Meikle, S., Yazici, Z., Eulitz, M., and Kolch, W. (2002) *EMBO J.* **21,** 64–71
63. Moelling, K., Schad, K., Bosse, M., Zimmermann, S., and Schweneker, M. (2002) *J. Biol. Chem.* **277,** 31099–31106
64. Hatakeyama, M., Kimura, S., Naka, T., Kawasaki, T., Yumoto, N., Ichikawa, M., Kim, J. H., Saito, K., Saeki, M., Shirouzu, M., Yokoyama, S., and Konagaya, A. (2003) *Biochem. J.* **373,** 451–463
65. Kotani, K., Yonezawa, K., Hara, K., Ueda, H., Kitamura, Y., Sakaue, H., Ando, A., Chavanieu, A., Calas, B., and Grigorescu, F. (1994) *EMBO J.* **13,** 2313–2321
66. Keely, P. J., Westwick, J. K., Whitehead, I. P., Der, C. J., and Parise, L. V. (1997) *Nature* **390,** 632–636
67. Chausovsky, A., Tsarfaty, I., Kam, Z., Yarden, Y., Geiger, B., and Bershadsky, A. D. (1998) *Mol. Biol. Cell* **9,** 3195–3209
68. Chausovsky, A., Waterman, H., Elbaum, M., Yarden, Y., Geiger, B., and Bershadsky, A. D. (2000) *Oncogene* **19,** 878–888
69. Reif, K., Nobes, C. D., Thomas, G., Hall, A., and Cantrell, D. A. (1996) *Curr. Biol.* **6,** 1445–1455
70. Carpenter, C. L., Tolias, K. F., Couvillon, A. C., and Hartwig, J. H. (1997) *Adv. Enzyme Regul.* **37,** 377–390
71. Adam, L., Vadlamudi, R., Kondapaka, S. B., Chernoff, J., Mendelsohn, J., and Kumar, R. (1998) *J. Biol. Chem.* **273,** 28238–28246
72. Kapeller, R., Toker, A., Cantley, L. C., and Carpenter, C. L. (1995) *J. Biol. Chem.* **270,** 25985–25991
73. Kobayashi, M., Nagata, S., Kita, Y., Nakatsu, N., Ihara, S., Kaibuchi, K., Kuroda, S., Ui, M., Iba, H., Konishi, H., Kikkawa, U., Saitoh, I., and Fukui, Y. (1997) *J. Biol. Chem.* **272,** 16089–16092
74. Kita, Y., Kimura, K. D., Kobayashi, M., Ihara, S., Kaibuchi, K., Kuroda, S., Ui, M., Iba, H., Konishi, H., Kikkawa, U., Nagata, S., and Fukui, Y. (1998) *J. Cell Sci.* **111,** 907–915
75. Stover, D. R., Becker, M., Liebetanz, J., and Lydon, N. B. (1995) *J. Biol. Chem.* **270,** 15591–15597
76. Juang, S. H., Carvajal, M. E., Whitney, M., Liu, Y. C., and Carraway, C. (1996) *Oncogene* **12,** 1033–1042
77. Pleiman, C. M., Hertz, W. M., and Cambier, J. C. (1994) *Science* **263,** 1609–1612